



**QUEEN'S
UNIVERSITY
BELFAST**

Microfluidic encapsulation method to produce stable liposomes containing lohexol

Delama, A., Teixeira, M. I., Dorati, R., Genta, I., Conti, B., & Lamprou, D. (2019). Microfluidic encapsulation method to produce stable liposomes containing lohexol. *Journal of Drug Delivery Science and Technology*, 54, [101340].

Published in:
Journal of Drug Delivery Science and Technology

Document Version:
Peer reviewed version

Queen's University Belfast - Research Portal:
[Link to publication record in Queen's University Belfast Research Portal](#)

Publisher rights

Copyright 2019 Elsevier.

This manuscript is distributed under a Creative Commons Attribution-NonCommercial-NoDerivs License (<https://creativecommons.org/licenses/by-nc-nd/4.0/>), which permits distribution and reproduction for non-commercial purposes, provided the author and source are cited.

General rights

Copyright for the publications made accessible via the Queen's University Belfast Research Portal is retained by the author(s) and / or other copyright owners and it is a condition of accessing these publications that users recognise and abide by the legal requirements associated with these rights.

Take down policy

The Research Portal is Queen's institutional repository that provides access to Queen's research output. Every effort has been made to ensure that content in the Research Portal does not infringe any person's rights, or applicable UK laws. If you discover content in the Research Portal that you believe breaches copyright or violates any law, please contact openaccess@qub.ac.uk.

1 **Microfluidic encapsulation method to produce stable liposomes containing Iohexol**

2 **Anna Delama^{1,2}, Maria Inês Teixeira^{1,3}, Rossella Dorati², Ida Genta², Bice Conti^{2,*} and Dimitrios**

3 **A. Lamprou^{1*}**

4 ¹ School of Pharmacy, Queen’s University Belfast, Belfast BT9 7BL, UK.

5 ² Department of Drug Sciences, University of Pavia, Viale Taramelli 12, 27100 Pavia, Italy.

6 ³ UCIBIO - REQUIMTE, Laboratory of Pharmaceutical Technology, Department of Drug Sciences,
7 Faculty of Pharmacy, University of Porto, Rua de Jorge Viterbo Ferreira, 228, 4050-313 Porto,
8 Portugal.

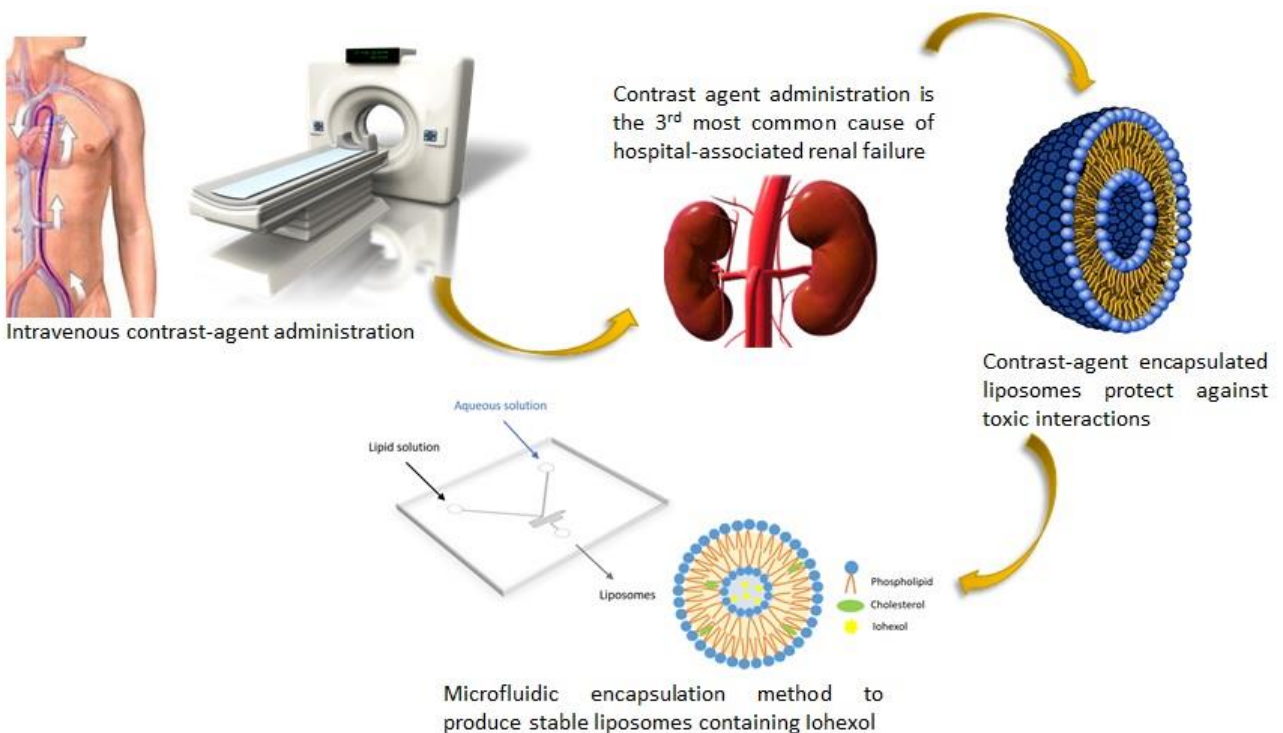
9 *Correspondence: D.A. Lamprou, E-mail address: D.Lamprou@qub.ac.uk, Tel.: +44-(0)28-9097-
10 2617. B. Conti, E-mail: bice.conti@unipv.it, Tel.: +39-0382-987378

11

12 **Keywords:** contrast media; Iohexol; liposomes; medical imaging; microfluidics.

13

14 **Graphical Abstract**



15

16 **ABSTRACT**

17 Since the discovery of X-rays in the late 1890s, several medical imaging techniques have been
18 developed, such as Computed Tomography (CT), Magnetic Resonance Imaging (MRI) and
19 Ultrasound Imaging, which are used daily to diagnose, monitor, or treat medical conditions. Some
20 of these techniques include the use of contrast agents to enhance the contrast images, therefore,
21 toxic effects must be considered. Among these, Contrast-Induced Nephropathy (CIN) is an acute
22 renal failure resulting from the administration of iodinated contrast media (CM). To date, there is
23 no definitive treatment for CIN and several prevention approaches have been evaluated.
24 Nanoparticles (NPs) represent a promising strategy for treatment and prevention of CIN, due to
25 their ability to deliver CM during diagnosis imaging. In this study, iohexol-containing liposomes were
26 produced using microfluidic technique for first time. Several phosphocholine lipids (e.g. DMPC,
27 DOPC, DPPC and DSPC) with cholesterol (2:1 ratio) were investigated and DLS, FTIR and *in vitro*
28 release studies at 37°C were performed, with stability studies conducted on the best formulation.
29 The microfluidic method allowed to obtain a high encapsulation efficiency (over 70%), and release
30 profiles showed an iohexol release around or less than 0.12 mg ml⁻¹ after 2 h for the majority of the
31 formulations, which is not toxic to the kidney cells.

32 **1. INTRODUCTION**

33 Nephropathy is the term used to describe any disease-causing damage to the small blood vessels or
34 blood cleaning apparatus in the kidneys, and often is an associated kidney complication of some
35 other disease or conditions, such as immunoglobulin A (IgA) nephropathy and Contrast-induced
36 nephropathy (CIN). There are certain situations where the interaction of a pharmaceutical agent,
37 upon administration to a patient, should ideally be hindered or even prevented completely.

38 CIN is reversible acute renal failure, which is the result of unwanted interactions between
39 radiocontrast-media (RCM) and the renal filtration system [1]. Several types of contrast media are

40 in use in medical imaging (X-ray attenuation: Iodine and barium; Magnetic resonance signal
41 enhancing: gadolinium; Ultrasound scattering and frequency shift: micro-bubble contrast agents)
42 and they can roughly be classified based on the imaging modalities where they are used. Moreover,
43 it is the third cause of hospital acquired acute renal failure and can lead to many adverse outcomes
44 including dialysis and increased mortality. CIN is one of the main causes of acute kidney injury (AKI)
45 and this is associated with high healthcare costs, long hospitalization and increased morbidity and
46 mortality [2]. Many risk factors are related to CIN and the most important is pre-existing severe
47 renal insufficiency. Other risk factors have been reported, such as diabetes, old age, gender,
48 hypertension or hyperuricemia, but not all of them have been rigorously confirmed [1]. Moreover,
49 CM with high osmolarity and viscosity can increase the incidence of CIN and the injected volume of
50 CM and the route of administration must be taken into account [3]. CIN occurs in 1.0% - 15% of all
51 patients undergoing invasive angiographic procedures and in 50% of patients with pre-existing renal
52 insufficiency or diabetes mellitus. The incidence is estimated to be about 7.0% - 11%, but rises up
53 to 40% in patients with chronic kidney disease (CKD) [2, 4]. To date, there is no definitive treatment
54 for CIN and several prevention approaches have been evaluated. Briefly, the strategies adopted for
55 preventing toxic effects are volume expansion (hydration), administration of antioxidants such as
56 N-Acetyl Cysteine, ascorbic acid and statins and, eventually, hemofiltration [1-3]. However, these
57 approaches are not yet supported by clinical evidence and they require critical medical care and
58 special treatments that are not always practical [2, 5].

59 For the reasons stated above, further approaches to prevent CIN should be evaluated. Under these
60 approaches belongs also the use of Nanoparticles (NPs), which represent a promising strategy for
61 prevention of CIN, due to their ability to deliver CM during diagnosis imaging, thus avoiding the
62 adverse reactions associated with these compounds [6]. Accordingly, several iodine-NPs have been
63 developed. However, there are some issues that currently limit the application of iodinated NPs *in*

64 *vivo* such as loading efficiency and burst release [7]. Furthermore, high concentrations of CM
65 incorporated are often required to improve imaging, causing an alteration in the NPs
66 physicochemical properties and *in vivo* behaviour [8]. Various approaches and compositions are
67 being investigated, such as iodinated polymeric micelles, where iodine was covalently linked to the
68 polymeric molecule to form micelles as blood pool agent (BPA) (Hallouard et al., 2010), [10, 11].
69 However, the major drawback of polymeric micelles is their thermodynamic instability after
70 intravenous administration, due to dilution below the critical micelle concentration of the polymer.
71 This causes dissociation of the micelle structure and release of the CM [12]. Polymeric NPs that have
72 been investigated as blood pool contrast agents includes the use of poly(L-lactide) (PLA), poly
73 (lactide-co-glycolide) (PLGA) or poly(ϵ -caprolactone) (PCL), thanks to their biocompatibility in terms
74 of acceptable shelf-life and non-toxic degradation products in case of metabolization [9, 13].
75 Moreover, iodinated dendrimers have been developed with a PEG-core and non-ionic contrast
76 agents covalently fixed onto the surface, but their synthesis is time-consuming [9]. Other
77 approaches consist in the production of lipid-based NPs such as liposomes that, thanks to their
78 structure, presenting a hydrophobic and a hydrophilic region, may incorporate both lipophilic and
79 hydrophilic CM. Moreover, iodine may be covalently incorporated into the lipid bilayer structure
80 with a modified phospholipid, by following examples of lipid formulation with CM as a carrier [9, 13,
81 14]. In addition, nanoemulsions have been developed and two formulations of 1,3-disubstituted
82 polyiodinated triglycerides (ITG) are commercially available [9, 13].

83 In this study, the focus is the use of phospholipids in the production of NPs loaded with iohexol since
84 liposomes have several properties that make them more advantageous than other drug delivery
85 systems, such as polymeric nanocarriers. First, their phospholipidic bilayer reproduces the cell
86 membrane structure, resulting in high biocompatibility. Furthermore, liposomes can be eliminated
87 from the body without any toxic effects via the reticuloendothelial system, thus avoiding renal

88 filtration and reducing nephrotoxicity associated to the CM. Liposomes, are the most common and
89 well-investigated nanocarriers and they may be synthesized from clinically approved components
90 (lipids and CM) with easy preparation methods. In addition, liposomes show several advantages of
91 high target accumulation and cellular uptake [11, 15-18].

92 The most commonly used method in literature for producing liposome is film hydration method
93 given that it is simple, convenient and widely applicable, but it has several limitations such as control
94 of the process and scalability, low encapsulation efficiency and time [18, 19]. Thus, in order to
95 overcome these issues, many novel technologies have been applied, such as microfluidics.
96 Microfluidics allow precise control over a fluid stream in contrast to the chaotic flows that occur in
97 the traditional method, since it is not governed by the same laws applied at the macroscale
98 techniques [20]. Among the microfluidics technologies, the microfluidic hydrodynamic focusing
99 (MHF) approach has been developed by Jahn *et al.* [21] for liposome production. Typically, a stream
100 of lipid in alcohol solution flows in the central channel of the device, while an aqueous solution flows
101 through two lateral channels (**Fig. 1**). In this way, the stream of lipids is hydrodynamically focused
102 by the two aqueous streams into the narrow junction of the chip. Thus, liposomes are formed due
103 to the diffusion of different molecular species at the liquid interface between the alcohol and the
104 aqueous phases: the two phases diffuse one into the other, causing the lipids' precipitation to form
105 micelles first and liposomes after. The easy control and adjustment of the flow rate ratio (FRR)
106 between the lipid and aqueous phase streams and the total flow rate (TFR), allow producing
107 uniformly dispersed liposomes. In particular, it has been reported that the mean diameter is directly
108 related to lipid concentration and inversely related to FRR. In addition, the device geometry has
109 been reported to affect the liposome characteristics [22, 23]. In conclusion, microfluidic methods
110 allow reaching a higher control over the physical properties of the final NPs: MHF allows obtaining
111 homogeneous vesicles in terms of size and lamellarity in one-step, unlike film hydration method

112 that requires additional processing steps, such as extrusion or ultrasonication, resulting in non-
113 uniform vesicles. Furthermore, this technique shows advantages, such as higher encapsulation
114 efficiency and reproducibility, even in large a scale for production of personalized products [23].
115 The aim of this proof of concept research was to produce liposomes for the prevention of CIN by
116 microfluidics. As CM, iohexol was selected, since it is a small water-soluble contrast agent that is
117 currently used for several radiographic procedures. The first goal, and novelty, was to obtain lipid
118 CM-loaded NPs using microfluidics, since to the best of our knowledge, there are no reports in the
119 literature. Formulation efforts were focused on obtaining a non-leakage of the iohexol in order to
120 avoid the toxic effects associated to the CM, such as CIN. Furthermore, it the achievement of a good
121 encapsulation efficiency was also intended.

122 **2. MATERIALS AND METHODS**

123 **2.1 Materials**

124 The synthetic lipids (**Fig. 2**) 1,2-dimyristoyl-sn-glycero-3-phosphocholine (DMPC), 1,2-Dioleoyl-sn-
125 Glycero-3-Phosphocholine (DOPC), 1,2-dipalmitoyl-sn-glycero-3-phosphocholine (DPPC), 1,2-
126 distearoyl-sn-glycero-3-phosphocholine (DSPC), cholesterol, iohexol (MW 821.14 Da, Water
127 Solubility 0.796 mg/mL, logP -3.05), tablets of phosphate-buffered saline (PBS, pH 7.4) and ethanol
128 $\geq 99.8\%$ were all obtained from Sigma-Aldrich.

129 **2.2 Preparation of liposomes by Microfluidics**

130 Liposomes were prepared using a microfluidic micro-mixer, which through hydrodynamic flow
131 enables nanoprecipitation of lipids. The Dolomite Microfluidics System was used, connected to a
132 Microfluidic cartridge with dimensions of 52 mm thick and 36 mm height with moulded channels of
133 300 μm in width and 130 μm in height with staggered herringbone structure. The mixing chips
134 consist of two stream inlets that merge into a micro-channel (**Fig. 3**). Lipids (DMPC, DOPC, DPPC,
135 DSPC) in combination with cholesterol (2:1 ratio) were dissolved in ethanol at a concentration of 5

136 mg/mL; the 2:1 ratio was chosen as has been previously reported to be the most stable ratio for the
137 specific lipid formulations [24]. The lipid solution was introduced in one of the inlet of the
138 microfluidics micro-mixer and the aqueous buffer (PBS, pH 7.4) or the iohexol solution (0.714 mg/mL
139 in water) in the other one. Both fluids were delivered into the chip inlets with two pressure pumps
140 with respective fluidic connections using FEP tubing of OD 1/16 and ID 250 μm . The TFR and the FRR
141 were controlled using two MitoS Flow Rate Sensors (0.2-5 mL min^{-1}). TFR of 1 mL min^{-1} and FRR
142 (lipid:aqueous phase) 3:1 were chosen, since this combination gave the best results (data not
143 included).

144 **2.3. Dynamic light scattering (DLS)**

145 The size distribution (mean diameter and PDI) of the liposomes was measured by Dynamic Light
146 Scattering (DLS) on a NanoBrook Omni (Brookhaven Instruments, Holtsville, NY, USA). Each sample
147 was measured three times at 25°C with a fixed angle of 90° in a dilution of 1:100 using PBS pH 7.4.
148 Moreover, the same instrument was used to measure the ζ -potential. For each formulation three
149 cycles of ζ -potential measurements were performed. Size and ζ distribution was measured in
150 multiple samples from each batch.

151 **2.4. Encapsulation efficiency and Release studies**

152 The most common method for study the release from NPs is dynamic dialysis [25]. Two release
153 studies were conducted for each formulation. Prior to the analysis, the dialysis tube (Dialysis tubing
154 cellulose membrane, Avg. flat width 10 mm, 0.4 in., MWCO 14,000, Sigma-Aldrich) was placed in
155 boiling water for 30 min and thoroughly rinsed with water. A volume of 1 mL of each liposome
156 suspension was added into the dialysis tube with both ends tied and the tube was suspended in PBS
157 10 mL at pH 7.4 and kept at 37.0 \pm 0.5°C for removal of unencapsulated CM for 1 h [26]. Then, 10 mL
158 of PBS was removed and kept for encapsulation efficiency analysis. The PBS was replaced with fresh
159 PBS pre-equilibrated at 37.0 \pm 0.5°C and CM release was analysed by extraction of 500 μL aliquots of

160 the PBS at intervals of 15 and 30 min and 1, 2, 4, 6, 24 h. The supernatant was replaced with fresh
161 PBS pre-equilibrated at 37°C at each time point, in order to satisfy sink conditions and keeping the
162 volume constant. The amount of drug released at each time point was determined by UV-vis
163 spectrophotometer (FLUOstar Omega, BMG LABTECH).

164 The concentration of non-encapsulated or released CM was determined with the aid of a calibration
165 curve of iohexol in purified water ($R^2 = 1$) at wavelength of maximum absorbance of iohexol (245
166 nm). The Equation used is: Iohexol Concentration (mg/mL) = (Absorbance – 0.0043) / 20.897.

167 The encapsulation efficiency was calculated using eq. 1:

$$168 \quad \% EE = ((C_i - C_{n.e.}) / C_i) \times 100 \quad (1)$$

169 where C_i is the initial concentration of iohexol added during preparation and $C_{n.e.}$ is the
170 concentration of iohexol non-encapsulated.

171 Release curves were drawn according to the cumulative drug release and plotted vs time using eq.
172 2.

$$173 \quad \% \text{ Cumulative Iohexol Release}_t = ((C_t / C_e) / v) \times 100 \quad (2)$$

174 where C_t is the concentration released at time t and in each previous time point, C_e is the
175 concentration of iohexol encapsulated ($C_e = C_i - C_{n.e.}$) and v is the volume of the aliquot of each
176 sample (0.5 mL).

177 **2.5. Fourier transform infrared spectroscopy (FTIR)**

178 All the excipients, including the lipids (DMPC, DOPC, DPPC and DSPC), cholesterol and iohexol were
179 analysed separately with infrared (IR). The liposome suspensions were scanned in an inert
180 atmosphere over a wave range of 4000–650 cm^{-1} over 32 scans at a resolution of 4 cm^{-1} and an
181 interval of 1 cm^{-1} . All FTIR spectra were recorded on a Spectrum Two (PerkinElmer) FT-IR
182 spectrometer using a MIRacle (PIKE Technologies) ATR accessory. The background was subtracted
183 from each spectrum.

184 **2.6. Stability studies**

185 The stability studies were conducted for four weeks after the preparation of the lipid
186 nanoformulation. The liposome batch was divided in two aliquots and kept at $5.0\pm 0.5^{\circ}\text{C}$ and at
187 $37.0\pm 0.5^{\circ}\text{C}$. Particle size and ζ -potential were measured at day 0, day 3 and after 1, 2, 3 and 4 weeks
188 from the preparation of liposomes.

189 **2.7 Statistical analysis**

190 All experiments were performed with calculation of means and standard deviations. Two-way
191 analysis of variance (ANOVA) was used for multiple comparisons. Significance was acknowledged
192 for p values lower than 0.05.

193 **3. RESULTS**

194 **3.1. Particle Sizing and Encapsulation efficiency**

195 Several phosphocholine lipids (e.g. DMPC, DOPC, DPPC and DSPC) were investigated using a
196 combination of 2:1 ratio with cholesterol since it is the most frequently and most stable
197 lipid:cholesterol ratio used in literature [24]. TFR 1 mL min^{-1} and FRR (lipid:aqueous phase) 3:1 were
198 settled, shown good particle size and polydispersity index (PDI; **Table 1**). Results in terms of particle
199 size and encapsulation efficiency are shown in **Fig. 4**. Empty liposomes were also produced, and
200 particle size, ζ -potential, and PDI were recorded (**Table 1**).

201 **3.2. Release Studies**

202 Release profiles of DMPC and DSPC formulations showed a leakage of iohexol less than 20% after 2
203 h, while DOPC and DPPC formulations released $22.43 \pm 0.64\%$ and $28.14 \pm 6.57\%$, respectively (**Fig.**
204 **5a**). After 24 h, around 50% of iohexol was released by all the formulations, except for the DMPC
205 formulation that showed a lower leakage of $25.69 \pm 1.26\%$ (**Fig. 5b**). After 24 h the studies were
206 stopped, given that was most important to observe the release after 2 h, which is the elimination
207 half-life of the CM [27]. Moreover, in all cases the release after 6 h was followed by a plateau phase.

208 3.3. FTIR Studies

209 FTIR was performed for the iohexol-loading liposomes, since the resulting spectrum acts as a
210 fingerprint for the compounds. All the excipients such as cholesterol, iohexol and lipids (DMPC,
211 DOPC, DPPC and DSPC) were analysed separately. In all the liposome spectra (**Fig. 6**) the broad band
212 detected at about 3300 cm^{-1} is related to O-H stretching of the hydroxyl groups present in
213 cholesterol and in iohexol molecules. The band at about 2900 cm^{-1} represents C-H stretching, while
214 the weak band detected at around 1700 cm^{-1} only in DOPC:Chol (2:1) formulation spectrum,
215 represents the stretching of carbonyl groups of the esters present in the lipid. The presence of
216 iohexol into the liposome is confirmed by the weak band at around 1600 cm^{-1} that represents C=O
217 stretching of the amidic groups. Finally, the strong band at about 1000 cm^{-1} represents the
218 stretching of the C-O bond [28]. Moreover, the lipid structure was not affected by the presence of
219 the iohexol since all the liposome spectra exhibited the peaks related to the groups of the lipid
220 molecules analysed separately (data not included).

221 3.4. Stability studies

222 Since the DOPC:Chol formulation showed the smallest particle size and good results in terms of
223 iohexol encapsulation efficiency and release, it was submitted to stability studies for four weeks at
224 $5\pm 0.5^\circ\text{C}$ and $37\pm 0.5^\circ\text{C}$, with no statistical differences between the two temperatures (**Fig. 7**). At day
225 0, it showed a mean diameter of $178.11 \pm 2.43\text{ nm}$ and ζ -potential value $-8.08 \pm 14.71\text{ mV}$. The
226 formulation stored at 5°C showed a good stability profile after 28 days, with small-reduced size
227 ($142.88 \pm 0.45\text{ nm}$). The formulation kept at $37\pm 0.5^\circ\text{C}$, follow the patent of the 5°C , except at 14
228 days that show a decreased in size ($126.79 \pm 3.88\text{ nm}$) and increased in ζ -potential absolute value
229 ($-9.05 \pm 1.4\text{ mV}$), however after 4 weeks it showed a mean diameter of $132.78 \pm 2.66\text{ nm}$.

230

231

232 **4. DISCUSSION**

233 The microfluidic method allowed obtaining a high encapsulation efficiency, more than 70% for all
234 the formulations. To our knowledge, any studies about iodinated NPs production by microfluidics
235 have not been reported in literature. However, these results confirm the advantages of microfluidic
236 technique since in the literature, the highest encapsulation efficiency that was reported is no more
237 than 25% for iohexol-containing liposomes prepared with the extrusion method using DPPC,
238 cholesterol and PEG2000-DSPE [15, 29, 30]. Furthermore, a drug loading of 30% was obtained for
239 multilamellar liposomes (MLVs), given that a larger size allows for a higher drug loading capacity
240 [31]. Moreover, DPPC, cholesterol and PEG, have been used for preparing liposomes loaded with
241 iodixanol, which is a non-ionic dimer CM more hydrophilic than the iohexol. Even in this case, the
242 extrusion method has been used and an encapsulation efficiency of only 25% was observed [32, 33].
243 In conclusion, these results confirmed that the encapsulation properties depend closely on the
244 experimental conditions [12] and that microfluidics allows to overcome limitations of batch
245 methods in terms of encapsulation efficiency.

246 Moreover, a mean diameter < 200 nm (177.64 ± 0.97 nm), that is fundamental to avoid a rapid RES
247 uptake, was obtained for the DOPC:Chol formulation with an encapsulation efficiency of $68.45 \pm$
248 3.41% . The release profile showed a leakage of $22.42 \pm 0.64\%$ after 2 h that should be rapidly
249 eliminated *in vivo*, since the elimination half-life of the free iohexol in patients with normal renal
250 function is 1 - 2 h [27]. Stability studies of the DOPC:Chol formulation showed that it might be stored
251 at 5°C for 1 month without significant changes in particle size.

252 **5. CONCLUSIONS**

253 In this study, we formulated iohexol-loading liposomes with high encapsulation efficiency and low
254 release. The microfluidic method allows preparing formulations under a well-controlled process
255 with reduced time and solvent waste, confirming the benefits of this technique. Microfluidics will

256 play a crucial role in the dawn of personalized medicine and in our case, for patients that cannot
257 receive CM due to pre-existing severe renal insufficiency and other risk factors of CIN.

258 **6. FUTURE DIRECTIONS**

259 As for future perspectives, in order to improve the release profile and to achieve specific target
260 tissue, the surface of the NPs may be modified to include polyethylene glycol (PEG), which is a
261 hydrophilic compound that can also prolong time circulation and stability of liposomes [30, 34, 35].
262 In fact, the use of a contrast agent with a long vascular residence time can be necessary in long
263 scanning time procedures. Eventually, thanks to the microfluidic technique, simple scalability may
264 be carried out for the production of personalized products. In fact, microfluidics offers easy scale-
265 up maintaining high resolution and sensitivity, decreasing cost production and time and, for these
266 reasons, microfluidics has the potential to become widely used because it is economical,
267 reproducible and, furthermore, can be integrated with other technologies [36, 37]. In particular, it
268 is possible to parallelize individual setup units to increase the total output of the systems, while
269 maintaining the advantages of microfluidics without altering the final characteristics of the NPs [38].
270 Such parallel approaches have already been studied for emulsion droplet production and polymeric
271 NPs [39]. However, the scale-up is still an active area of research for chemical engineering since it
272 requires not only architecture and materials able to support higher internal pressure, but also that
273 the system setup can ensure the same operating conditions during the process [39, 40].

274 **ACKNOWLEDGMENTS**

275 The authors would like to thank the ERASMUS+ programme for the mobile scholarships to A.D. and
276 M.I.T.

277 **CONFLICTS OF INTEREST**

278 The authors declare no conflict of interest.

279 REFERENCES

- 280 [1] C. Mamoulakis; K. Tsarouhas; I. Fragkiadoulaki; I. Heretis; M.F. Wilks; D.A. Spandidos; C. Tsitsimpikou; A.
281 Tsatsakis, Contrast-induced nephropathy: Basic concepts, pathophysiological implications and
282 prevention strategies. *Pharmacol Ther.* 180, (2017), 99-
283 112. <https://doi.org/10.1016/j.pharmthera.2017.06.009>
- 284 [2] A. Ali; C. Bhan; M.B. Malik; M.Q. Ahmad; S.A. Sami, The Prevention and Management of Contrast-
285 induced Acute Kidney Injury: A Mini-review of the Literature. *Cureus.* 10, (2018),
286 e3284.10.7759/cureus.3284
- 287 [3] A.-L. Faucon; G. Bobrie; O. Clément, Nephrotoxicity of iodinated contrast media: from pathophysiology
288 to prevention strategies. *Eur J Radiol.* (2019). <https://doi.org/10.1016/j.ejrad.2019.03.008>
- 289 [4] L. Azzalini; V. Spagnoli; H.Q. Ly, Contrast-Induced Nephropathy: From Pathophysiology to Preventive
290 Strategies. *Can J Cardiol.* 32, (2016), 247-255. <https://doi.org/10.1016/j.cjca.2015.05.013>
- 291 [5] N.M.A. Mohammed; A. Mahfouz; K. Achkar; I.M. Rafie; R. Hajar, Contrast-induced Nephropathy. *Heart*
292 *Views.* 14, (2013), 106-116.10.4103/1995-705X.125926
- 293 [6] N. Naseri; E. Ajorlou; F. Asghari; Y. Pilehvar-Soltanahmadi, An update on nanoparticle-based contrast
294 agents in medical imaging. *Artif Cells Nanomed Biotechnol.* 46, (2018), 1111-
295 1121.10.1080/21691401.2017.1379014
- 296 [7] Y. Ding; X. Zhang; Y. Xu; T. Cheng; H. Ou; Z. Li; Y. An; W. Shen; Y. Liu; L. Shi, Polymerization-induced self-
297 assembly of large-scale iohexol nanoparticles as contrast agents for X-ray computed tomography
298 imaging. *Polym Chem.* 9, (2018), 2926-2935.10.1039/C8PY00192H
- 299 [8] L. Arms; D.W. Smith; J. Flynn; W. Palmer; A. Martin; A. Woldu; S. Hua, Advantages and Limitations of
300 Current Techniques for Analyzing the Biodistribution of Nanoparticles. *Front Pharmacol.* 9, (2018),
301 802-802.10.3389/fphar.2018.00802
- 302 [9] F. Hallouard; N. Anton; P. Choquet; A. Constantinesco; T. Vandamme, Iodinated blood pool contrast
303 media for preclinical X-ray imaging applications – A review. *Biomaterials.* 31, (2010), 6249-
304 6268. <https://doi.org/10.1016/j.biomaterials.2010.04.066>
- 305 [10] M. Shilo; T. Reuveni; M. Motiei; R. Popovtzer, Nanoparticles as computed tomography contrast agents:
306 current status and future perspectives. *Nanomedicine.* 7, (2012), 257-269.10.2217/nnm.11.190
- 307 [11] D.P. Cormode; P.C. Naha; Z.A. Fayad, Nanoparticle contrast agents for computed tomography: a focus
308 on micelles. *Contrast Media Mol Imaging.* 9, (2014), 37-52.10.1002/cmml.1551
- 309 [12] J. Siepmann; A. Faham; S.-D. Clas; B.J. Boyd; V. Jannin; A. Bernkop-Schnürch; H. Zhao; S.
310 Lecommandoux; J.C. Evans; C. Allen; O.M. Merkel; G. Costabile; M.R. Alexander; R.D. Wildman; C.J.
311 Roberts; J.-C. Leroux, Lipids and polymers in pharmaceutical technology: Lifelong companions. *Int J*
312 *Pharm.* 558, (2019), 128-142. <https://doi.org/10.1016/j.ijpharm.2018.12.080>
- 313 [13] H. Lusic; M.W. Grinstaff, X-ray-computed tomography contrast agents. *Chem Rev.* 113, (2013), 1641-
314 1666.10.1021/cr200358s
- 315 [14] N. Lee; S.H. Choi; T. Hyeon, Nano-Sized CT Contrast Agents. *Adv Mater.* 25, (2013), 2641-
316 2660.10.1002/adma.201300081
- 317 [15] S.J. Burke; A. Annapragada; E.A. Hoffman; E. Chen; K.B. Ghaghada; J. Sieren; E.J.R. van Beek, Imaging of
318 Pulmonary Embolism and t-PA Therapy Effects Using MDCT and Liposomal Iohexol Blood Pool Agent:
319 Preliminary Results in a Rabbit Model. *Acad Radiol.* 14, (2007), 355-362.10.1016/j.acra.2006.12.014
- 320 [16] M. Silindir; S. Erdogan; A.Y. Ozer; S. Maia, Liposomes and their applications in molecular imaging. *J*
321 *Drug Target.* 20, (2012), 401-415.10.3109/1061186x.2012.685477
- 322 [17] L. Sercombe; T. Veerati; F. Moheimani; S.Y. Wu; A.K. Sood; S. Hua, Advances and Challenges of
323 Liposome Assisted Drug Delivery. *Front Pharmacol.* 6, (2015), 286-286.10.3389/fphar.2015.00286
- 324 [18] Y. Xia; C. Xu; X. Zhang; P. Ning; Z. Wang; J. Tian; X. Chen, Liposome-based probes for molecular
325 imaging: from basic research to the bedside. *Nanoscale.* 11, (2019), 5822-5838.10.1039/C9NR00207C
- 326 [19] A. Akbarzadeh; R. Rezaei-Sadabady; S. Davaran; S.W. Joo; N. Zarghami; Y. Hanifehpour; M. Samiei; M.
327 Kouhi; K. Nejati-Koshki, Liposome: classification, preparation, and applications. *Nanoscale Res Lett.* 8,
328 (2013), 102-102.10.1186/1556-276X-8-102

- 329 [20] E. Chiesa; R. Dorati; S. Pisani; B. Conti; G. Bergamini; T. Modena; I. Genta, The Microfluidic Technique
330 and the Manufacturing of Polysaccharide Nanoparticles. *Pharmaceutics*. 10, (2018),
331 267.10.3390/pharmaceutics10040267
- 332 [21] A. Jahn; W.N. Vreeland; M. Gaitan; L.E. Locascio, Controlled vesicle self-assembly in microfluidic
333 channels with hydrodynamic focusing. *J Am Chem Soc*. 126, (2004), 2674-2675.10.1021/ja0318030
- 334 [22] B. Yu; R.J. Lee; L.J. Lee, Microfluidic methods for production of liposomes. *Methods Enzymol*. 465,
335 (2009), 129-141.10.1016/S0076-6879(09)65007-2
- 336 [23] D. Carugo; E. Bottaro; J. Owen; E. Stride; C. Nastruzzi, Liposome production by microfluidics: potential
337 and limiting factors. *Sci Rep*. 6, (2016), 25876-25876.10.1038/srep25876
- 338 [24] M.-L. Briuglia; C. Rotella; A. McFarlane; D.A. Lamprou, Influence of cholesterol on liposome stability
339 and on in vitro drug release. *Drug Deliv Transl Res*. 5, (2015), 231-242.10.1007/s13346-015-0220-8
- 340 [25] S. Modi; B.D. Anderson, Determination of Drug Release Kinetics from Nanoparticles: Overcoming
341 Pitfalls of the Dynamic Dialysis Method. *Mol Pharm*. 10, (2013), 3076-3089.10.1021/mp400154a
- 342 [26] M. Guimarães Sá Correia; M.L. Briuglia; F. Niosi; D.A. Lamprou, Microfluidic manufacturing of
343 phospholipid nanoparticles: Stability, encapsulation efficacy, and drug release. *Int J Pharm*. 516,
344 (2017), 91-99.<https://doi.org/10.1016/j.ijpharm.2016.11.025>
- 345 [27] D.C. Wymer, CHAPTER 5 - Imaging, in: 2010. in: Floege J., Johnson R.J., Feehally J. (Eds.),
346 *Comprehensive Clinical Nephrology (Fourth Edition)*, Mosby, 2010, p. 56-74.
- 347 [28] P. Larkin, Chapter 6 - IR and Raman Spectra-Structure Correlations: Characteristic Group Frequencies,
348 in: 2011. in: Larkin P. (Eds.), *Infrared and Raman Spectroscopy*, Elsevier, 2011, p. 73-115.
- 349 [29] C.Y. Kao; E.A. Hoffman; K.C. Beck; R.V. Bellamkonda; A.V. Annapragada, Long-residence-time nano-
350 scale liposomal iohexol for X-ray-based blood pool imaging. *Acad Radiol*. 10, (2003), 475-483
- 351 [30] J. Zheng; G. Perkins; A. Kirilova; C. Allen; D.A. Jaffray, Multimodal Contrast Agent for Combined
352 Computed Tomography and Magnetic Resonance Imaging Applications. *Invest Radiol*. 41, (2006),
353 339-348.10.1097/01.rli.0000186568.50265.64
- 354 [31] W. Xiaohui; G. Fang; H. Dandan; Q. Jian; X. Yuhong. Liposomal Contrast Agent for CT Imaging of the
355 Liver. 2005 IEEE Engineering in Medicine and Biology 27th Annual Conference; 2005 17-18 Jan. 2006.
- 356 [32] S. Mukundan; K.B. Ghaghada; C.T. Badea; C.-Y. Kao; L.W. Hedlund; J.M. Provenzale; G.A. Johnson; E.
357 Chen; R.V. Bellamkonda; A. Annapragada, A Liposomal Nanoscale Contrast Agent for Preclinical CT in
358 Mice. *AJR Am J Roentgenol*. 186, (2006), 300-307.10.2214/AJR.05.0523
- 359 [33] C.T. Badea; K.K. Athreya; G. Espinosa; D. Clark; A.P. Ghafoori; Y. Li; D.G. Kirsch; G.A. Johnson; A.
360 Annapragada; K.B. Ghaghada, Computed Tomography Imaging of Primary Lung Cancer in Mice Using
361 a Liposomal-Iodinated Contrast Agent. *PLOS ONE*. 7, (2012), e34496.10.1371/journal.pone.0034496
- 362 [34] P.T. Vladimir, Polymeric Contrast Agents for Medical Imaging. *Curr Pharm Biotechnol*. 1, (2000), 183-
363 215.<http://dx.doi.org/10.2174/1389201003378960>
- 364 [35] M.L. Immordino; F. Dosio; L. Cattel, Stealth liposomes: review of the basic science, rationale, and
365 clinical applications, existing and potential. *International journal of nanomedicine*. 1, (2006), 297-315
- 366 [36] P.M. Valencia; O.C. Farokhzad; R. Karnik; R. Langer, Microfluidic technologies for accelerating the
367 clinical translation of nanoparticles. *Nature nanotechnology*. 7, (2012), 623-
368 629.10.1038/nnano.2012.168
- 369 [37] N. Forbes; M.T. Hussain; M.L. Briuglia; D.P. Edwards; J.H.t. Horst; N. Szita; Y. Perrie, Rapid and scale-
370 independent microfluidic manufacture of liposomes entrapping protein incorporating in-line
371 purification and at-line size monitoring. *International Journal of Pharmaceutics*. 556, (2019), 68-
372 81.<https://doi.org/10.1016/j.ijpharm.2018.11.060>
- 373 [38] A. Bohr; S. Colombo; H. Jensen, Chapter 15 - Future of microfluidics in research and in the market, in:
374 2019. in: Santos H.A., Liu D., Zhang H. (Eds.), *Microfluidics for Pharmaceutical Applications*, William
375 Andrew Publishing, 2019, p. 425-465.
- 376 [39] J.-M. Lim; N. Bertrand; P.M. Valencia; M. Rhee; R. Langer; S. Jon; O.C. Farokhzad; R. Karnik, Parallel
377 microfluidic synthesis of size-tunable polymeric nanoparticles using 3D flow focusing towards in vivo
378 study. *Nanomedicine*. 10, (2014), 401-409.<https://doi.org/10.1016/j.nano.2013.08.003>
- 379 [40] M.K. Mulligan; J.P. Rothstein, Scale-up and control of droplet production in coupled microfluidic flow-
380 focusing geometries. *Microfluid Nanofluidics*. 13, (2012), 65-73.10.1007/s10404-012-0941-7

381 **Table & Figure Captions**

382 **Table 1:** Mean particle size, polydispersity index (PDI) and ζ -potential of different liposome
383 formulations without iohexol.

384 **Figure 1:** Schematic representation of liposome formation by microfluidic hydrodynamic focusing
385 (MHF) method.

386 **Figure 2:** Chemical structures of: a) 1,2-dimyristoyl-sn-glycero-3-phosphocholine (DMPC), b) 1,2-
387 Dioleoyl-sn-Glycero-3-Phosphocholine (DOPC), c) 1,2-dipalmitoyl-sn-glycero-3-phosphocholine
388 (DPPC), d) 1,2-distearoyl-sn-glycero-3-phosphocholine (DSPC), e) Cholesterol and f) Iohexol.

389 **Figure 3:** Representation of microfluidic chip for the production of lipid nanoformulations.

390 **Figure 4:** Mean particle size (bars, left axis) (n=3, p value=0.0007, PDI DMPC:Chol 0.293, PDI
391 DOPC:Chol 0.261, DPPC:Chol 0.300, DSPC:Chol 0.220) and percentage encapsulation efficiency
392 (dots, right axis) (n=2, p value=0.01) of different liposome formulations.

393 **Figure 5:** Cumulative drug release studies over time, of different liposome formulations: a) in the
394 first 2h, and b) after 24 hours (n=2, p value=0.04).

395 **Figure 6:** FTIR spectra of different liposome formulations: a) DMPC:Chol, b) DOPC:Chol, c)
396 DPPC:Chol, and d) DSPC:Chol.

397 **Figure 7:** a) Mean particle size (p value 5°C=0.00000002, p value 37°C=0.0000009) and b) ζ -potential
398 (p value 5°C=0.07, p value 37°C=0.06) of DOPC:Chol loading iohexol formulation (n=3).

399

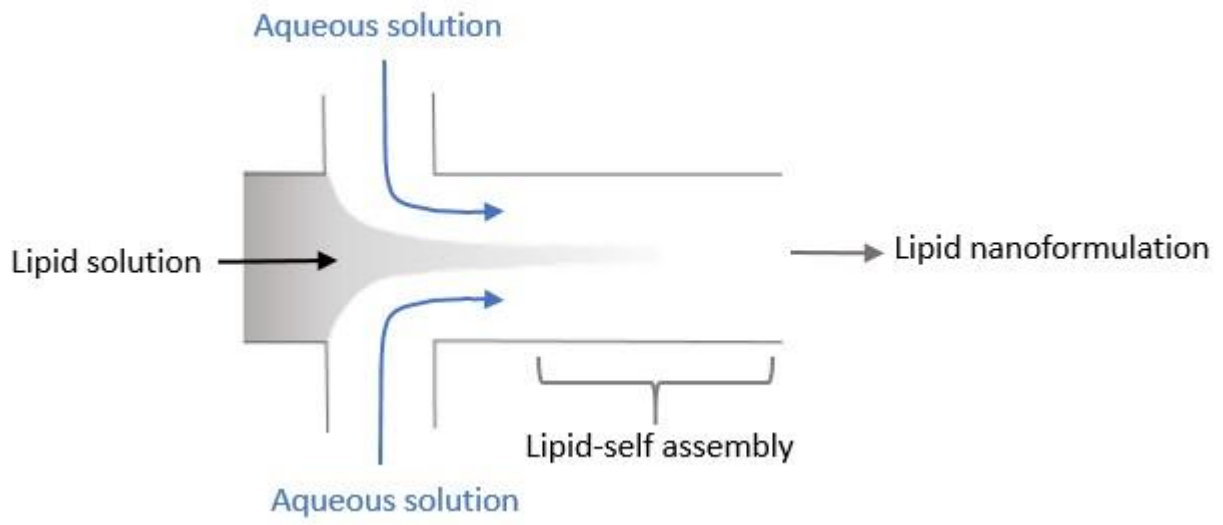
400 **Table 1:**

Formulation	Mean diameter / nm	PDI	ζ-potential / mV
DMPC:Chol	435.02 ± 28.44	0.310	-2.33 ± 7.01
DOPC:Chol	132.25 ± 4.29	0.240	-27.76 ± 5.78
DPPC:Chol	416.31 ± 20.91	0.258	-1.91 ± 8.65
DSPC:Chol	671.42 ± 102.13	0.222	-10.60 ± 6.28

401

402

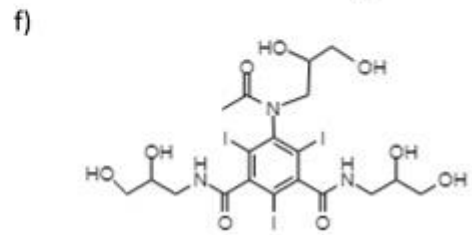
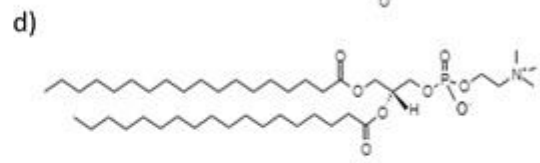
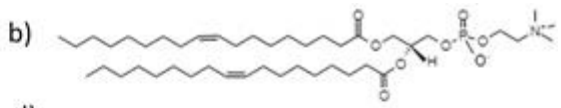
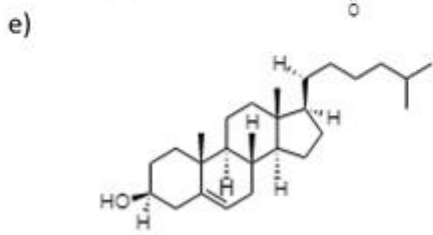
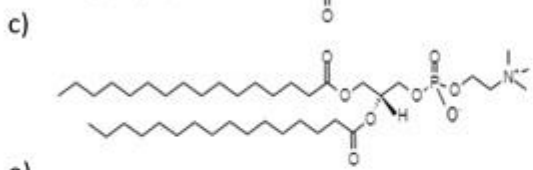
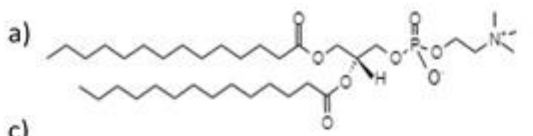
403 **Figure 1:**



404

405

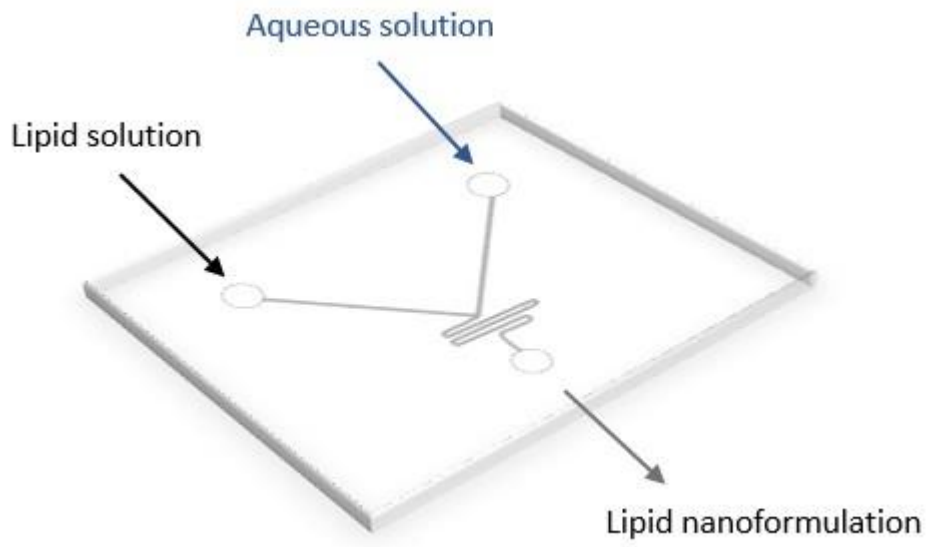
406 **Figure 2:**



407

408

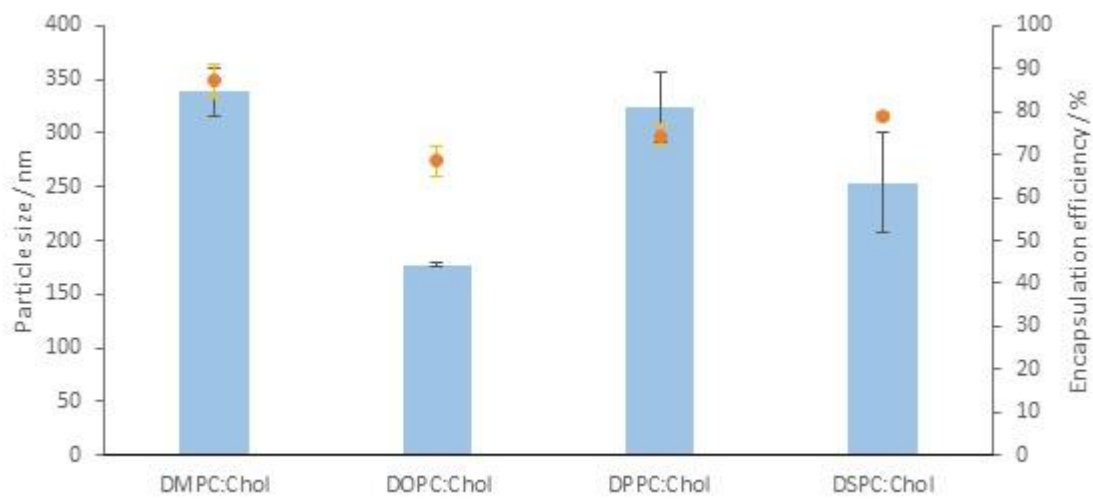
409 **Figure 3:**



410

411

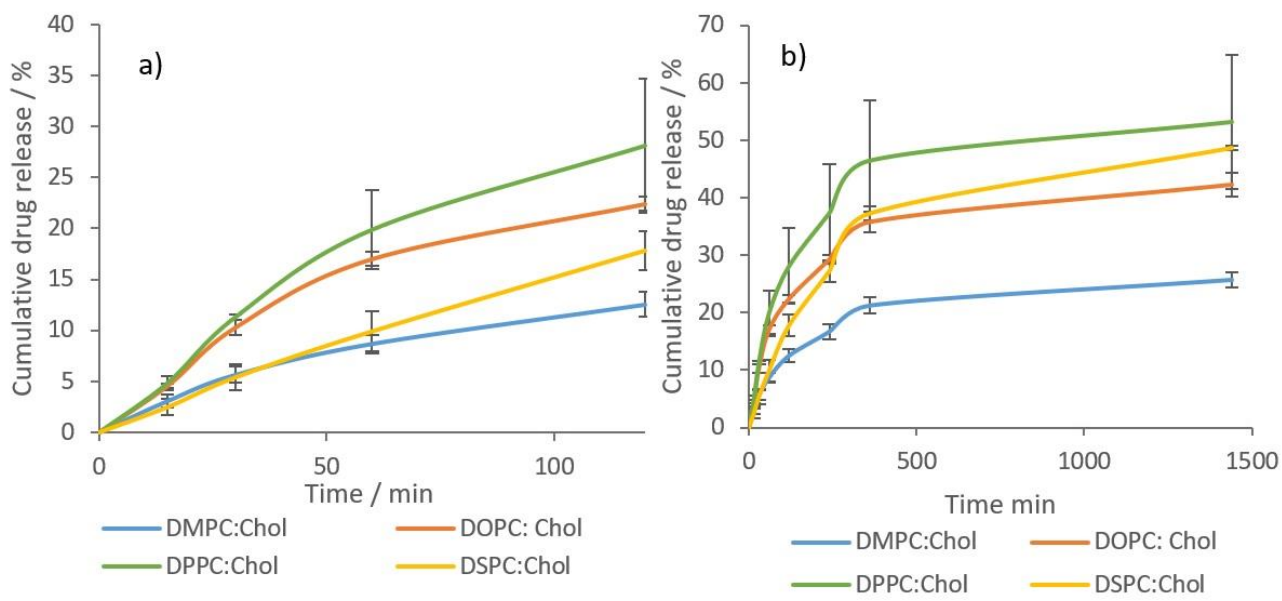
412 **Figure 4:**



413

414

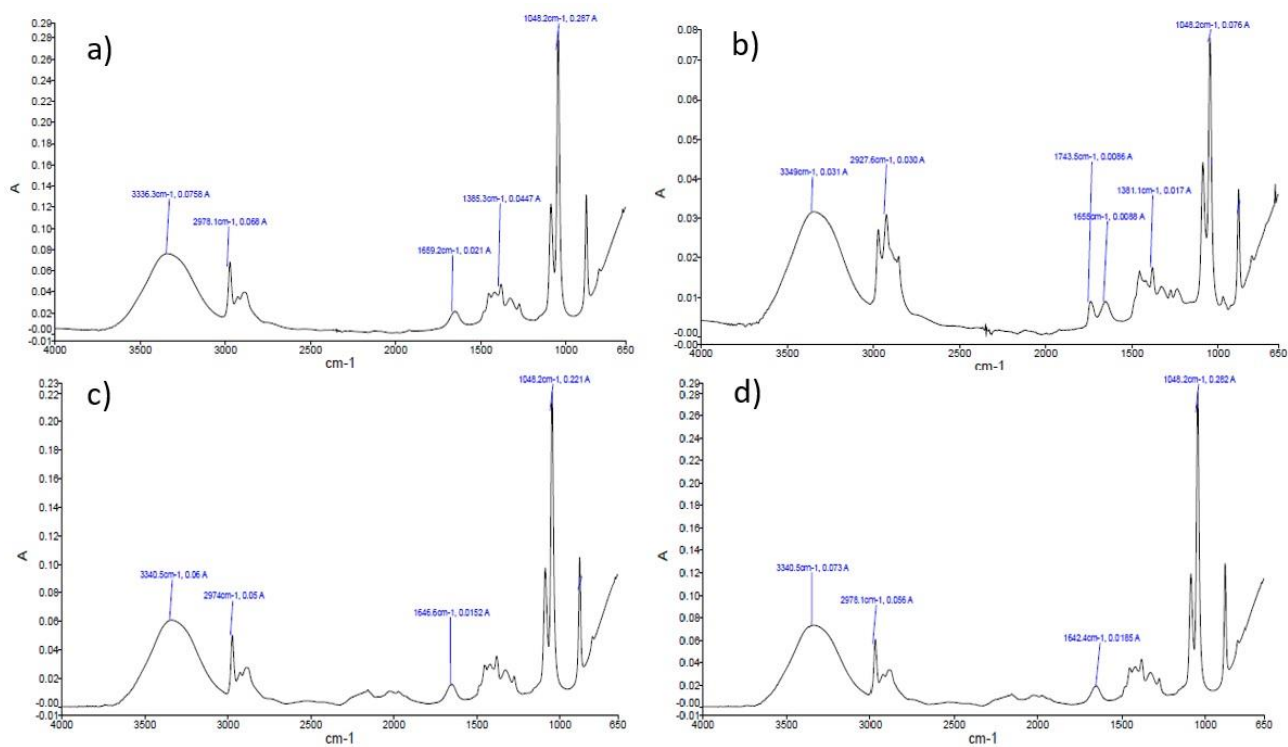
415 **Figure 5:**



416

417

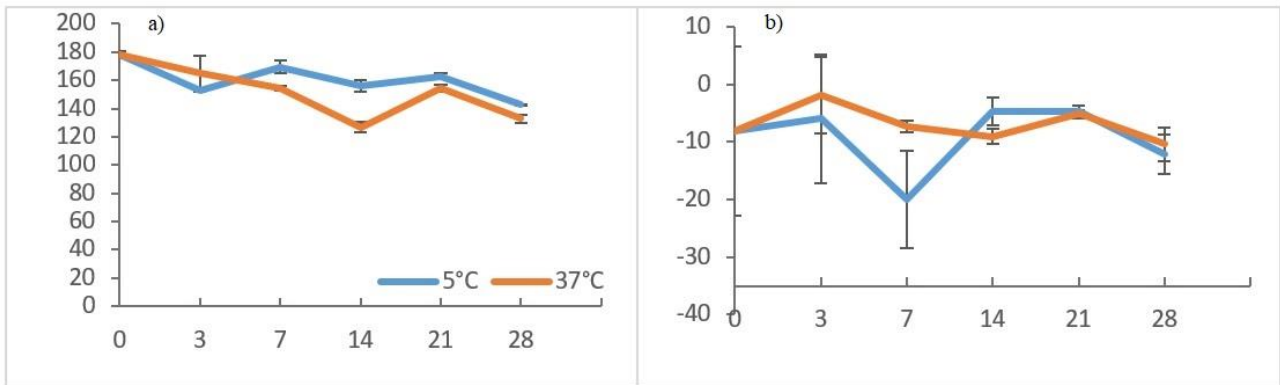
418 **Figure 6:**



419

420

421 **Figure 7:**



422